Fiber-feedback continuous-wave and synchronously-pumped singly-resonant ring optical parametric oscillators using reverse-proton-exchanged periodically-poled lithium niobate waveguides

Carsten Langrock* and M. M. Fejer

Edward L. Ginzton Laboratory, Stanford University, Stanford, California 94305-4085, USA
**Corresponding author: langrock@stanford.edu*

Received March 19, 2007; accepted May 21, 2007;
posted May 29, 2007 (Doc. ID 81245); published July 30, 2007

We describe guided-wave singly-resonant reverse-proton-exchanged (RPE) periodically-poled lithium niobate (PPLN) waveguide ring optical parametric oscillators (OPOs) in which the feedback was provided via a single-mode fiber pigtailed to the waveguide. Wavelength selection was achieved by means of a fiber Bragg grating inside the feedback loop. The SRO threshold for the synchronously-pumped OPO was below 1 mW of average coupled pump power. © 2007 Optical Society of America

OCIS codes: 190.4970, 190.4390.

Optical parametric oscillators (OPOs) are flexible coherent light sources based on parametric interactions inside a nonlinear crystal between a strong pump and the subsequently generated signal–idler pair ($\omega_{\text{pump}} = \omega_{\text{signal}} + \omega_{\text{idler}}$) inside a resonant cavity [1]. Since the pump power required to reach oscillation threshold (gain=loss, for a singly-resonant OPO (SRO)) decreases as the gain per unit input power increases, the large nonlinear susceptibility and tight confinement over long interaction lengths available in periodically-poled lithium niobate (PPLN) waveguides allows for low-threshold operation [2–5]. Previously demonstrated annealed-proton-exchanged PPLN waveguide OPOs have used linear standing-wave cavities either via external mirrors or dieletric coatings on the waveguide facets [2,3]. Low-threshold CW SROs as well as pulsed doubly-resonant OPOs (DROs) have been demonstrated using Ti-diffused PPLN waveguides [4,5]. These devices were pumped using C-band sources, generating mid-IR radiation.

The devices presented here represent fully-integrated CW and synchronously-pumped (synch-pumped) ring SROs using reverse-proton-exchanged (RPE) PPLN waveguides. Pump coupling as well as resonant feedback is provided via single-mode optical fiber (SMF) pigtailed to the waveguide devices. Resonant feedback via SMF was previously demonstrated in a synch-pumped bulk PPLN OPO [6]. The OPOs can be tuned over their parametric gain bandwidths via a frequency-selective element inside the feedback loop; >60 nm (>150 nm) tuning range was demonstrated around the 1558 nm (1550 nm) center wavelength for the CW (synch-pumped) OPO. While there are well-established sources available for C-band wavelengths, the device concept presented here can easily be extended to other wavelengths of interest.

A schematic of our experimental setups can be seen in Fig. 1(a). For the CW OPO, light from an external-cavity tunable diode laser running at 779 nm was coupled into a 67-mm-long RPE PPLN waveguide device containing a 49-mm-long QPM grating (16.1 μm period). The synch-pumped OPO used a mode-locked Ti:sapphire laser producing ~1 ps FWHM pulses at 775 nm with a repetition rate of 76 MHz as the pump source and a 29-mm-long RPE PPLN waveguide device containing a 11.5-mm-long QPM grating (16 μm period). To achieve synch-pumped operation, we added a fiber-coupled variable delay line to the feedback to synchronize the OPO's cavity length and repetition rate f_{rep} to those of the Ti:sapphire laser. For convenience, we chose a feedback length correspond-

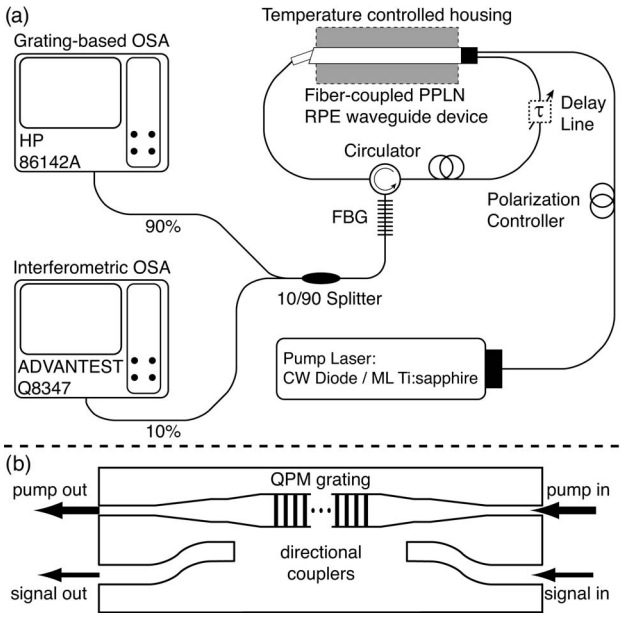

Fig. 1. (a) Experimental setup for CW and synch-pumped operation; the variable delay line is only present in the synch-pumped setup. (b) Schematic of the waveguide device with on-chip WDM and adiabatic tapers for mode matching to SMF.

0146-9592/07/152263-3/$15.00

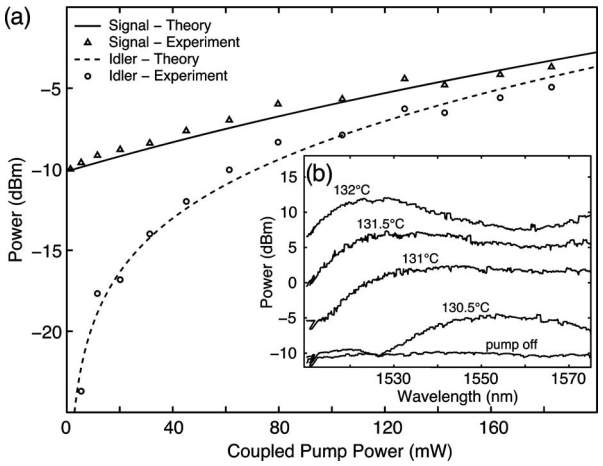

Fig. 2. (a) OPA signal and idler output power versus pump power. (b) OPA signal gain spectra at several crystal temperatures. Data were obtained using the OSA in peak-hold mode while scanning the signal laser; for clarity, the traces are offset along the ordinate.

ing to $f_{rep}/4$, which increased the average SRO threshold pump power by a factor of four over a length corresponding to f_{rep}.

The generated C-band signals were then coupled into a SMF at the output of the device via an on-chip wavelength-division multiplexer (WDM) as shown in Fig. 1(b). The WDM was required to ensure efficient launching of both the pump and the resonant C-band light. After passing through a frequency-selective element (here, a fiber Bragg grating (FBG) attached to a circulator), they were fed back into the waveguide's input via an identical WDM. Due to the use of nonpolarization-maintaining fiber, polarization controllers were added to the pump and the signal-return paths. Light not reflected by the FBG was split and monitored using a grating-based (HP 86142A) and an interferometric (Advantest Q8347) optical spectrum analyzer.

The initial characterization of the 67-mm-long RPE PPLN waveguide device for CW operation was performed via optical parametric amplification by opening the ring cavity and injecting light from a C-band external cavity diode laser and monitoring the amplified output signal as well as the generated idler frequency as a function of crystal temperature and pump power. The experimental results shown in Fig. 2 are in good agreement with numerical simulations and demonstrate the large parametric gain bandwidth (>60 nm) of this device.

After closing the ring cavity, SRO threshold was reached at a coupled pump power of approximately 200 mW. This threshold is set by loop losses such as the circulator (1.5 dB), waveguide-to-fiber coupling (0.7 dB signal input, 0.6 dB signal output), as well as waveguide propagation losses (α=0.2 dB/cm, 6.7 cm device length), and the normalized conversion efficiency [7] (η_{norm}=92%/W cm^2). In the limit of lossless propagation, undepleted pump, and zero phase mismatch, the single-pass signal gain can be expressed as $\eta=P_s(L)/P_s(0)=\cosh^2(\sqrt{\eta_{norm}P_{pump}})$. The theoretical SRO threshold was calculated to be 187 mW, following the analysis in [8]. This threshold can be as low as 64 mW, assuming currently best device parameters (η_{norm}=110%/W cm^2, α=0.1 dB/cm, 0.3 dB waveguide-to-fiber coupling loss per facet, 1 dB loss for in-loop components). As shown in Fig. 3(a), a small fraction of the resonant light at 1563 nm leaked through the FBG and could be monitored simultaneously with the nonresonant C-band signal at 1553 nm.

We observed single peaks at 1563 and 1553 nm on the interferometric OSA [shown in Fig. 3(b)]. Due to this optical spectrum analyzer's resolution bandwidth limit of 7 pm, we cannot claim single axial mode operation, even though it has been shown that ring OPOs frequently run on a single axial mode [9]. Due to the finite bandwidth of our FBG (0.2 nm, 3 dB bandwidth) and small crystal temperature fluctuations (±0.1°C), we observed a cyclic shift in oscillation frequency within the allowed bandwidth. Tuning of the oscillation frequency over the parametric gain bandwidth provided by the QPM structure can be achieved by replacing the fixed FBG with a tunable one. The DRO case has also been investigated by replacing the frequency-selective element with a power splitter. While the DRO threshold is significantly lower (~30 mW), stable operation has not been achieved at this point. Separation of the conjugate C-band signals and independent phase control would have to be implemented to improve DRO stability.

The initial open-loop characterization of the 29-mm-long RPE PPLN waveguide device for synch-pumped operation was performed by recording parametric fluorescence spectra at various temperatures to measure the parametric gain bandwidth. A bandwidth exceeding 150 nm was observed at a crystal temperature of 174°C.

After establishing feedback by closing the ring cavity and adjusting the delay line, we observed SRO operation at an average coupled pump power of approximately 3 mW. The threshold predicted for a feedback length corresponding to f_{rep} rather than $f_{rep}/4$ is less than 1 mW. Due to the dual-grating FBG (JDS Uniphase) used in this experiment, we observed

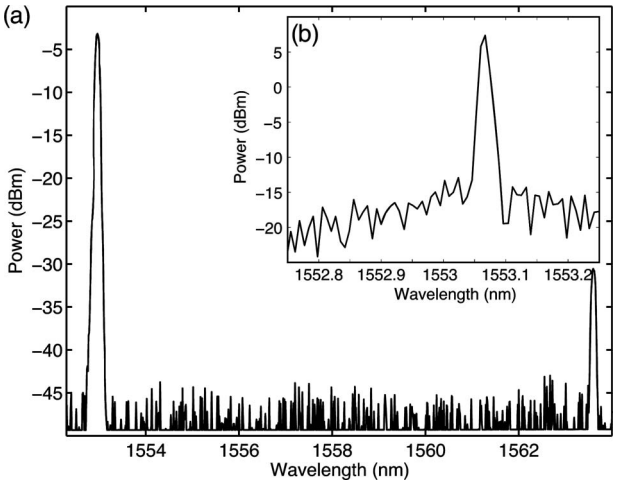

Fig. 3. (a) Grating-based OSA trace showing both resonated and outcoupled waves. (b) Interferometric OSA trace showing outcoupled wave at instrument's 7 pm resolution limit.

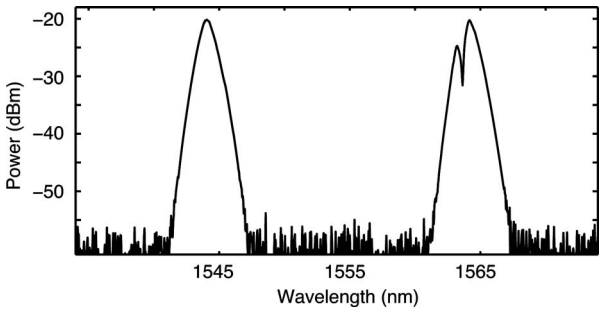

Fig. 4. OSA trace of synch-pumped OPO output spectrum showing two-color operation with 2 nm FWHM output pulses.

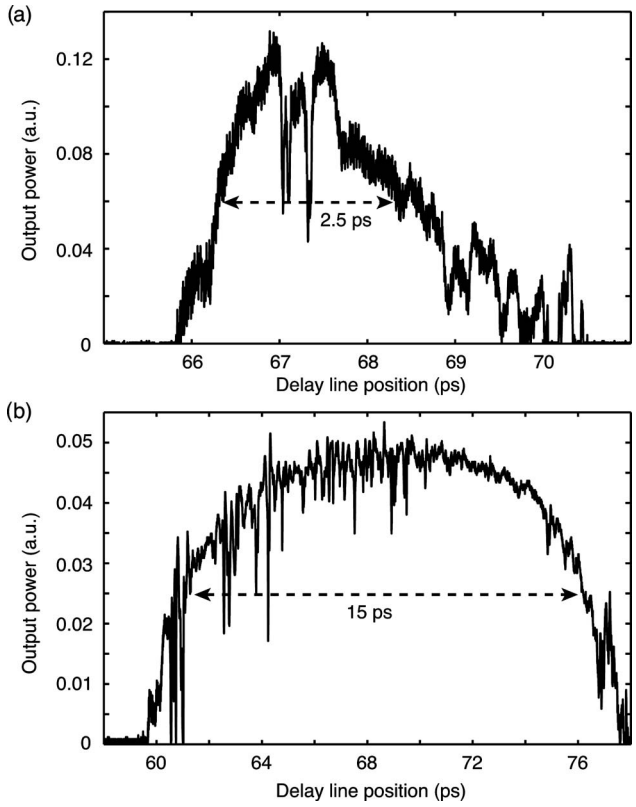

Fig. 5. (a) Synch-pumped OPO output power as a function of delay line position (a) near and (b) three times above SRO threshold.

two-color operation as shown in Fig. 4. This should not be mistaken for doubly-resonant operation. The generated C-band pulses had a spectral FWHM of 2 nm, which corresponds to that of a transform-limited 1.25 ps pulse, but no measurements of the pulse width were carried out.

We measured the synch-pumped OPO's output power dependence on delay line position at oscillation threshold and three times above it. Near threshold, operation could only be achieved in a relatively narrow delay range of 2.5 ps, corresponding to approximately twice the pump pulse duration [Fig. 5(a)]. This range was greatly increased above threshold [Fig. 5(b)], where stable SRO operation could be maintained over more than a 15 ps delay range. These results agree well with previous observations of bulk synch-pumped OPOs [6].

In conclusion, we have demonstrated alignment-free CW and picosecond synch-pumped PPLN waveguide SROs in a fiber-loop configuration. The CW (synch-pumped) SRO's parametric gain bandwidth exceeded 60 nm (150 nm), covering both the C- and the L-band. Other wavelength ranges can be accessed with minor changes to the current configuration. Tuning across the parametric gain bandwidth can be achieved via a simple in-line frequency-selective element. For operation a few times above threshold, the synch-pumped SRO was insensitive to cavity length fluctuations. We demonstrated two-color operation using a dual-grating FBG. Integration of the resonant feedback loop on-chip is possible by combining directional couplers and tight waveguide bends [10].

This research was sponsored by the MURI Center for Photonic Quantum Information Systems (Army Research Office/Advanced Research and Development Activity program DAAD19-03-1-0199), the Air Force Office of Scientific Research (AFOSR grant FA9550-05-1-0180), the Defense Advanced Research Projects Agency through the University of New Mexico Optoelectronic Materials Research Center (DARPA Prime MDA972-00-1-0024), and Crystal Technology, Inc.

References

1. S. E. Harris, Proc. IEEE **57**, 2096 (1969).
2. M. L. Bortz, M. A. Arbore, and M. M. Fejer, Opt. Lett. **20**, 49 (1995).
3. M. A. Arbore and M. M. Fejer, Opt. Lett. **22**, 151 (1997).
4. D. Hofmann, G. Gschreiber, W. Grundkotter, R. Ricken, and W. S. Sohler, presented at the Conference on Lasers and Electro-Optics Europe, Nice, France, September 10–15, 2000.
5. W. Sohler, W. Grundkötter, D. Hofmann, I. Kostjucenko, S. Orlov, V. Quiring, R. Ricken, G. Schreiber, and H. Suche, in *Conference on Lasers and Electro-Optics* (Optical Society of America, 2005).
6. T. Südmeyer, J. A. der Au, R. Paschotta, U. Keller, P. G. R. Smith, G. W. Ross, and D. C. Hanna, Opt. Lett. **26**, 304 (2001).
7. E. J. Lim, M. L. Bortz, and M. M. Fejer, Appl. Phys. Lett. **59**, 2040 (1991).
8. G. P. Bava, I. Montrosset, W. Sohler, and H. Suche, IEEE J. Quantum Electron. **QE-23**, 42 (1987).
9. W. R. Bosenberg, A. Drobshoff, J. I. Alexander, L. E. Myers, and R. L. Byer, Opt. Lett. **21**, 1336 (1996).
10. X. P. Xie, J. Huang, and M. M. Fejer, Opt. Lett. **31**, 2190 (2006).